Available online at www.sciencedirect.com

ScienceDirect

International Journal of Solids and Structures 45 (2008) 2671–2685

INTERNATIONAL JOURNAL OF SOLIDS AND STRUCTURES

www.elsevier.com/locate/ijsolstr

Physical and mechanical moisture susceptibility of asphaltic mixtures

N. Kringos [a,b,*], A. Scarpas [b]

[a] Faculty of Civil Engineering and Geosciences, TU Delft, Stevinweg 1, 2628 CN, Delft, The Netherlands
[b] Group of Mechanics of Structural Systems, Faculty of Civil Engineering and Geosciences, Delft University of Technology, The Netherlands

Received 5 August 2007; received in revised form 20 December 2007
Available online 4 January 2008

Abstract

Moisture has for a long time been recognized as a serious contributor to premature degradation of asphaltic pavements. Many studies have been performed to collect, describe and measure the moisture susceptibility of asphaltic mixes. Most of these aimed at a comparative measure of moisture damage, either via visual observations from field data or comparative laboratory tests. The research presented in this paper is part of an ongoing research effort to move away from such comparative or empirical measures of moisture induced damage of asphaltic materials and develop a fundamental approach via a comprehensive energy based computational framework. Such a framework would enable realistic predictions and time assessment of the failure pattern occurring in an asphaltic pavement under the given environmental and traffic loading, which could be rutting, cracking, raveling or any combination or manifestation thereof. The paper discusses the fundamental moisture induced damage parameters and demonstrates the developed model.

Keywords: Moisture damage; Asphaltic mixes; Energy based model; Elasto-visco-plastic large strains; Finite element modelling

1. Moisture induced damage in asphaltic pavements

Asphaltic mixes are a composition of aggregates and bituminous cement, in which the bituminous cement (named mastic) consists of bitumen, sand and fine filler particles and could include modifiers such as polymers, phosphoric acid or hydrated lime. In asphaltic pavements which are exposed to moisture infiltration, separation of the aggregates from the mix is a commonly encountered problem. The continuing action of moisture induced weakening and traffic load induced mechanical damage causes a progressive dislodgement of the aggregates and, in some cases, this damage pattern becomes a dominant mode of failure and a cause for diminished road safety. This damage phenomenon is known as *stripping* or *raveling* of the asphalt wearing surface and is contributed to a combined weakening of the mastic and a weakening of the aggregate–mastic bond. The

* Corresponding author. Address: Faculty of Civil Engineering and Geosciences, TU Delft, Stevinweg 1, 2628 CN, Delft, The Netherlands. Tel.: +31 152785519; fax: +31 152787313.
E-mail address: N.Kringos@TUDelft.nl (N. Kringos).

0020-7683/$ - see front matter
doi:10.1016/j.ijsolstr.2007.12.017

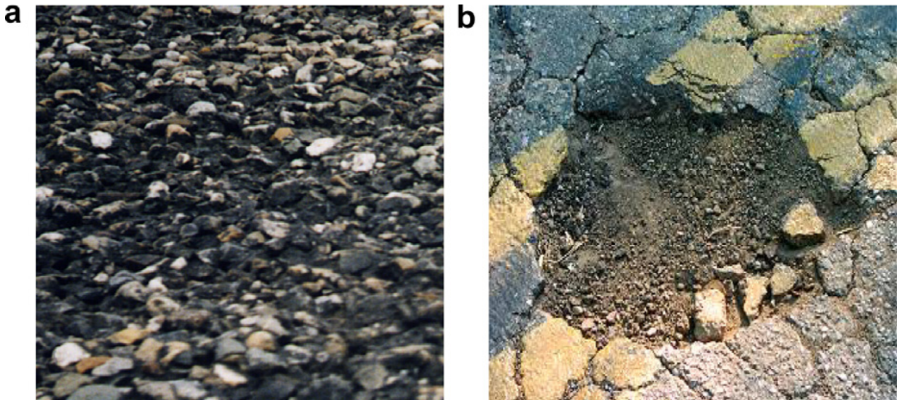

Fig. 1. Moisture induced damage in asphaltic pavements. (a) Raveling. (b) Pothole formation.

initial stripping damage can rapidly progress into a more severe degradation of the wearing surface, and ultimately lead to pothole formation (Fig. 1).

Over the years, many elaborate studies have been performed to study this topic (Curtis et al., 1991; Fromm, 1979; Graf, 1986; Hicks, 1991; Ishai and Craus, 1972; Kanitpong and Bahia, 2003; Kandhal, 1992, 1994, 2001; Lytton, 2002; Majidzadeh and Brovold, 1968; Mcgennis et al., 1984; Riedel and Weber, 1953; Scholz et al., 1993; Scott, 1978; Stuart, 1990; Takkalou, 1984; Taylor and Khosla, 1983), yet almost all of these studies aimed at a comparative measure of moisture damage, either via visual observations from field data or laboratory tests or via wet-versus-dry mechanical tests to give a so called moisture damage index parameter. Even though these tests seem to constitute a quick and simple way of comparing the moisture susceptibility of the mixes, they are highly subject to the boundary conditions of the experiment, they do not give any fundamental insight into the causes and evolution of the damage in time within the mix, nor can they directly be used for mix improvements. Given the fact that an asphalt mix is a composite material, which can have a wide range of properties and which may be compacted in various ways and levels, completely different material properties may result, each time an asphalt mix is produced and placed on the pavement. It would take an isolation of each possible variable to get any information regarding the controlling parameters, which is practically impossible in such empirical tests.

2. New approach towards characterizing and modelling moisture induced damage

Given this lack of tools which give a quantifiable fundamental knowledge of the causes and evolution of moisture induced damage, an extensive experimental and computational research program has been initiated in 2003 in the group of Mechanics of Structural Systems of Delft University of Technology, in the Netherlands, named RAVEMOD. The aim of this research program is to develop a more fundamental approach towards the identification and quantification of the moisture induced damage processes and their mechanical manifestations. The important starting point of this research is the conviction of the researchers that the problem of moisture induced damage in asphalt cannot be solved by mechanical considerations alone. It has been shown that, even without any mechanical loading, moisture has a degrading effect on the material properties. This implies that moisture makes a physical change to the material properties, which exhibits itself in the early development of damage patterns which, without the moisture, may have not occurred or may have occurred in a much later stage of the pavement's service life.

In this context, a new computational tool has been developed for the fundamental analysis of combined mechanical and moisture induced damage of asphaltic mixes which includes both physical and mechanical moisture damage inducing processes. The tool is named RoAM (Raveling of Asphaltic Mixes) (Kringos and Scarpas, 2005; Kringos, 2007), and is a sub-system of the large finite element system CAPA-3D (Scarpas, 2000, 2005).

In this paper, to indicate the importance of the various moisture sensitivity parameters on the overall response, the developed model is demonstrated on an idealized representation of an asphaltic mix. But first, in the following, the formulations of the wet and dry constitutive model are shown, followed by a description of the dominant moisture susceptibility parameters.

3. Energy based elasto-visco-plastic constitutive model

3.1. Combined physical–mechanical moisture induced damage processes

In this research, moisture induced damage processes are divided into physical and mechanical processes. The physical processes that are included as important contributors to moisture induced damage are (I) weakening of the mastic and the aggregate–mastic bond due to molecular diffusion of moisture and (II) weakening of the mastic from an erosion process of the mastic, caused by water flow (Fig. 2(a)). The mechanical damage process that is identified as a contributor to moisture damage is the occurrence of intense water pressure fields inside the mix caused by traffic loads and referred to as 'pumping action' (Fig. 2(b)).

These material degradation processes are integrated within the developed elasto-visco-plastic constitutive model for the resulting response of the material. Eventually, moisture induced damage will follow from the combined effect of the physical and mechanical moisture damage inducing processes, which result into a weakening of the mastic and a weakening of the aggregate–mastic bond (Fig. 2(c)).

In the following, the dry constitutive model is discussed, followed by the inclusion of the moisture induced damage processes.

3.2. Dry formulation

Mastic in asphalt mixes is known to be a material whose behaviour, depending on strain rate and temperature, exhibits response characteristics varying anywhere between the elasto-plastic and the visco-elastic limits. Constitutive models for such types of materials can be developed by combining the features of purely elasto-plastic and purely visco-elastic materials to create a more general category of constitutive models termed elasto-visco-plastic. Fig. 3 shows a one-dimensional schematic of the proposed material model consisting of a single elasto-plastic component in parallel with an arbitrary number of visco-elastic ones. The actual number of necessary components is to be decided on the basis of the available experimental evidence.

On the basis of energy arguments and by means of multiplicative decomposition of the deformation gradient tensor $\mathbf{F}$ into elastic and plastic $\mathbf{F} = \mathbf{F}_{\infty}\mathbf{F}_{p}$ or into elastic and viscous components $\mathbf{F} = \mathbf{F}_{e}\mathbf{F}_{v}$, a three-dimensional version of the above parallel model can be derived (Scarpas, 2005; Kringos et al., 2007a) (see Fig. 4).

To define the general framework of the energy based constitutive model, the Helmholtz free energy function is expressed as

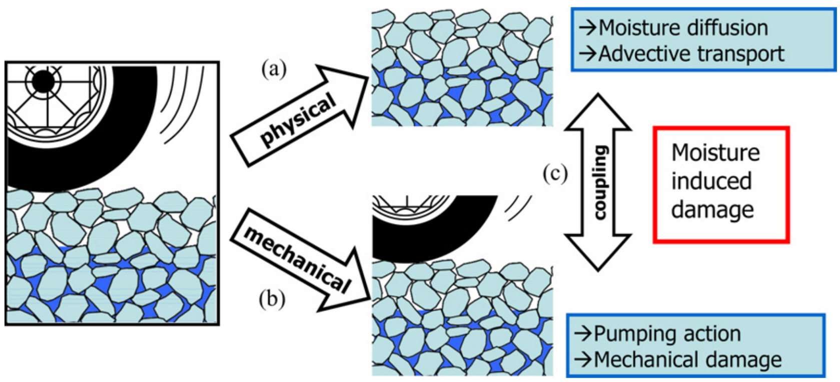

Fig. 2. Schematic of the new approach towards moisture induced damage.

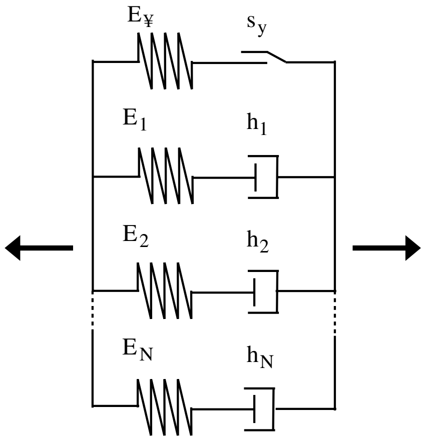

Fig. 3. One-dimensional representation of parallel elasto-visco-plastic material model.

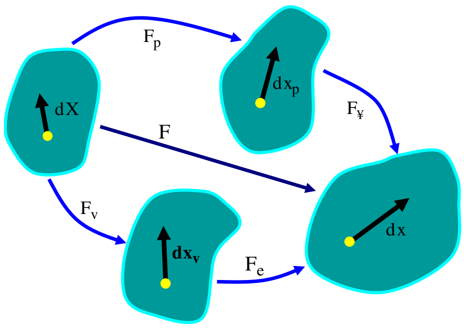

Fig. 4. Three-dimensional model for energy based elasto-visco-plastic material response.

$$\Psi = \Psi_{\mathrm{v}}(\mathbf{C}_{\mathrm{e}}) + \Psi_{\mathrm{p}}(\mathbf{C}_{\infty}, \xi_{\mathrm{p}}) \tag{1}$$

in which $\Psi_{\mathrm{v}}(\mathbf{C}_{\mathrm{e}})$ is the viscous strain energy function, $\mathbf{C}_{\mathrm{e}} = \mathbf{F}_{\mathrm{e}}^{\mathrm{T}}\mathbf{F}_{\mathrm{e}}$ is the Cauchy-Green strain tensor, based on the deformation gradient $\mathbf{F}_{\mathrm{e}}$, $\Psi_{\mathrm{p}}(\mathbf{C}_{\infty}, \xi)$ is the plastic free energy function, $\mathbf{C}_{\infty} = \mathbf{F}_{\infty}^{\mathrm{T}}\mathbf{F}_{\infty}$ is the Cauchy-Green strain tensor based on the deformation gradient $\mathbf{F}_{\infty}$ and ξ_{p} is the equivalent plastic strain.

From the second law of thermodynamics, the dissipation inequality can be found as

$$\mathbf{S} : \frac{1}{2}\dot{\mathbf{C}} - \left[\frac{\partial \Psi_{\mathrm{v}}}{\partial \mathbf{C}_{\mathrm{e}}} : \dot{\mathbf{C}}_{\mathrm{e}}\right] - \left[\frac{\partial \Psi_{\mathrm{p}}}{\partial \mathbf{C}_{\infty}} : \dot{\mathbf{C}}_{\infty} + \frac{\partial \Psi_{\mathrm{p}}}{\partial \xi_{\mathrm{p}}} \dot{\xi}_{\mathrm{p}}\right] \geqslant 0 \tag{2}$$

where $\mathbf{S}$ is the second Piola-Kirchhoff stress tensor. It can be shown that from the above inequality the stress tensor $\mathbf{S}$ can be additively decomposed into the visco-elastic $\mathbf{S}_{\mathrm{e}}$ and the elasto-plastic plastic component $\mathbf{S}_{\infty}$

$$\begin{aligned} \mathbf{S} &= 2\mathbf{F}_{\mathrm{v}}^{-1} \frac{\partial \Psi_{\mathrm{v}}}{\partial \mathbf{C}_{\mathrm{e}}} \mathbf{F}_{\mathrm{v}}^{-\mathrm{T}} + 2\mathbf{F}_{\mathrm{p}}^{-1} \frac{\partial \Psi_{\mathrm{p}}}{\partial \mathbf{C}_{\infty}} \mathbf{F}_{\mathrm{p}}^{-\mathrm{T}} \\ &= \mathbf{S}_{\mathrm{e}} + \mathbf{S}_{\infty} \end{aligned} \tag{3}$$

Furthermore, the following inequalities are obtained

$$2\mathbf{F}_{\mathrm{e}} \frac{\partial \Psi_{\mathrm{v}}}{\partial \mathbf{C}_{\mathrm{e}}} \mathbf{F}_{\mathrm{e}}^{\mathrm{T}} \mathbf{F}_{\mathrm{e}}^{-\mathrm{T}} : \mathbf{F}_{\mathrm{e}} l_{\mathrm{v}} \geqslant 0 \tag{4}$$

$$2\mathbf{F}_{\infty} \frac{\partial \Psi_{\mathrm{p}}}{\partial \mathbf{C}_{\infty}} \mathbf{F}_{\infty}^{\mathrm{T}} \mathbf{F}_{\infty}^{-\mathrm{T}} : \mathbf{F}_{\infty} l_{\mathrm{p}} - \frac{\partial \Psi_{\mathrm{p}}}{\partial \xi_{\mathrm{p}}} \dot{\xi}_{\mathrm{p}} \geqslant 0 \tag{5}$$

In the following, the dry constitutive model is adjusted to incorporate the moisture induced damage.

3.3. Wet formulation

To include moisture induced damage, a moisture damage parameter d_m is defined, which can be included into Eq. (1) as an internal variable, in addition to the strain tensors and the plastic damage:

$$\Psi_{md} = \Psi(\mathbf{C}_e, \mathbf{C}_\infty, \xi, d_m) = (1 - d_m)\Psi = (1 - d_m)[\Psi_v(\mathbf{C}_e) + \Psi_p(\mathbf{C}_\infty, \xi)] \tag{6}$$

Following the same procedure as above, but replacing the free energy function Ψ by the free energy function Ψ_{md} that is dependent also on moisture damage

$$\mathbf{S}_{md} : \frac{1}{2}\dot{\mathbf{C}} - \dot{\Psi}_{md} \geqslant 0 \tag{7}$$

Subsequently, the stress tensor can now be formulated as

$$\mathbf{S}_{md} = (1 - d_m)[\mathbf{S}_p + \mathbf{S}_v] \tag{8}$$

Also, on the basis of the maximum plastic dissipation principle, for the elasto-plastic component the following constrained system is obtained

$$\begin{aligned} l_p &= \lambda\left(\frac{\partial f}{\partial \mathbf{S}_{md}}\right) \\ \dot{\xi} &= \lambda\left(\frac{\partial f}{\partial q_{md}}\right) \\ \lambda \geqslant 0; &\quad f(\mathbf{S}_{md}, q_{md}) \leqslant 0; \quad \lambda f(\mathbf{S}_{md}, q_{md}) = 0 \end{aligned} \tag{9}$$

in which l_p is the plastic velocity gradient tensor, f is the yield surface, q is the conjugate to $\dot{\xi}$ thermodynamic force and λ is the plastic multiplier.

Similarly, for a visco-elastic component

$$l_v = \mathbb{C}_v^{-1} : \mathbf{S}_{md} \tag{10}$$

with

$$\mathbb{C}_v^{-1} = \frac{1}{2\eta_D}\left(\mathbb{I} - \frac{1}{3}\mathbf{I} \otimes \mathbf{I}\right) + \frac{1}{9\eta_V}\mathbf{I} \otimes \mathbf{I} \tag{11}$$

in which l_v is the viscous velocity gradient tensor and η_D and η_V are the deviatoric and volumetric viscosities (Reese and Govindjee, 1998). Detailed implementation procedures can be found in Scarpas and Kasbergen (2006).

3.4. Moisture flow and molecular diffusion

For the simulation of water infiltration into an asphaltic mix, two different phenomena need to be simulated. First of all, considering asphalt on a meso-level, the mix consists of a matrix of coated aggregates which have 'macro-pores' in between them. The infiltration of moisture into these macro-pores will be mainly dependent on hydraulic suction and flow velocity processes. Secondly, once the moisture has reached these macro-pores, the moisture may infiltrate further within the bulk materials of the aggregate–mastic matrix. This infiltration is, in contrast to the previous phenomenon, not a pressure driven process, but a molecular diffusion driven process which depends on a moisture concentration gradient in the material.

For the simulation of the water flow through the mix, assuming Darcy's law, the water velocity field can be described by

$$\operatorname{div}\mathbf{v} = -\tilde{\theta}\frac{\partial p}{\partial t} \tag{12}$$

where $\mathbf{v}$ is the water velocity, p is the water pressure and $\tilde{\theta}$ is the water capacity, equal to

$$\tilde{\theta} = \phi \frac{dS}{dp} \tag{13}$$

in which ϕ is the porosity and S the pressure dependent saturation.

For the simulation of the moisture diffusion into the asphalt mix components, a diffusion flux $\mathbf{J}_d$ of Fickean type is assumed:

$$\mathbf{J}_\mathrm{d} = -\mathbf{D}\nabla(C_\mathrm{m}) \tag{14}$$

where $\mathbf{D}$ is the molecular diffusion tensor $[L^2/T]$. More details on the computational scheme can be found in Kringos (2007) and Kringos et al. (2007b, 2008b).

4. Model parameters

4.1. Dry response

The parameters of the developed energy based elasto-visco-plastic constitutive model must be determined from experimental data. In collaboration with the University of Nottingham an extensive data-base has been developed which is used for the calibration and validation of the developed model. In Fig. 5 an example is given of the comparison between experimental results and computational predictions for a creep-recovery test in compression on an asphaltic sample.

As can be seen from the comparison, a good prediction of the first and secondary material response phase is found for both the axial and radial response (Kringos, 2007).

4.2. Moisture induced damage parameters

The physical moisture induced damage that is caused by the two types of moisture infiltration is also quite different. Depending on the overall mix permeability, a fast flow field may cause an erosion process of the mastic film, caused by a high velocity field in combination with weakened adsorption and dispersion characteristics of the film. The moisture diffusion into the asphalt components is a more gradual process, which drives the moisture into the asphalt components on a longer time scale and which will cause a gradual softening of the mastic and the aggregate–mastic bond.

In the developed model, the moisture sensitivity of the mix is governed by six fundamental material parameters, which are explained in the following.

Moisture can infiltrate into the asphalt mix components via diffusion through the mastic films or via hydraulic suction or pressure driven flow via the connected macro-pores. Moisture diffusion through the mastic is controlled by the diffusion coefficient D_mst. Depending on the sensitivity of the components to moisture, damage will occur to the mechanical material properties when moisture diffuses through its components. The moisture susceptibility of the mastic, the aggregate–mastic interface and the aggregates is covered by the

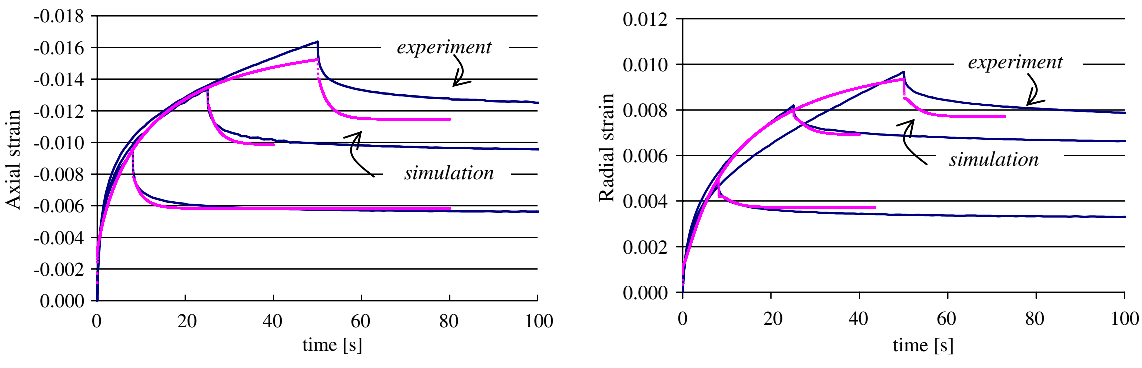

Fig. 5. Comparison model prediction with experimental data for a creep-recovery test.

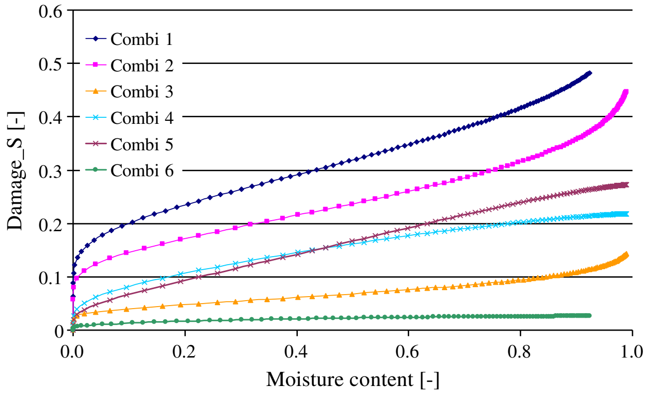

Fig. 6. Moisture induced damage of the mastic–aggregate interface as a function of moisture.

parameters $\alpha_\theta^{\rm mst}$, $\alpha_\theta^{\rm if}$ and $\alpha_\theta^{\rm stone}$, respectively. The water flow through the macro-pores may cause an erosion of the mastic films, which is covered by the desorption coefficient $K_{\rm d}^{\rm mst}$. Due to the erosion, the density of the mastic will reduce and the mechanical properties will change. The relationship between the mechanical properties of the mastic and its density is controlled by the moisture susceptibility parameter $\alpha_{\hat\rho}^{\rm mst}$. These six parameters are then expressed into two types of moisture damage functions.

To formulate the damage within the asphalt mix components, due to an increased moisture concentration θ, a Kachnov like damage parameter is defined which can go from 0 (no moisture damage) to 1 (complete moisture damage):

$$d_\theta^\kappa = f_\theta(D_{\rm k}, \alpha_\theta^\kappa) \quad \kappa = {\rm mst,\ if,\ stone} \tag{15}$$

where the function f_θ has to satisfy $f_\theta = 0.0$ for $\theta = 0.0$ and $f_\theta \leqslant 1.0$ for $\theta = 1.0$. This relationship must be determined experimentally for all the asphalt components, i.e. the mastic, the aggregate and the aggregate–mastic interface (Copeland et al., 2007).

In Fig. 6 a few examples of the experimentally determined $d_\theta^{\rm if}$ function are given (Kringos et al., 2008a). From the graphs it becomes clear how diverse the moisture susceptibility of the aggregate–mastic bond can be.

The second physical moisture induced damage parameter is postulated for the mastic component, which is based on the erosion of the mastic due to a water flow field:

$$d_{\hat\rho}^{\rm mst} = 1 - f_{\hat\rho}(K_{\rm d}, \alpha_{\hat\rho}^{\rm mst}) \tag{16}$$

with

$$\hat\rho(x,t) = \frac{\rho(x,t)}{\rho_0}; \quad 0.0 \leqslant \hat\rho \leqslant 1.0 \tag{17}$$

where ρ_0 is the undamaged mastic density and $\rho(x,t)$ is the updated mastic density. The function $f_{\hat\rho}$ has to satisfy $f_{\hat\rho} = 1.0$ for $\hat\rho = 1.0$ and $f_{\hat\rho} = 0.0$ for $\hat\rho = 0.0$, and should only be determined for the mastic.

The two damage processes can be represented by the damage parameter $d_{\rm m}$ in Eq. (6), which follows from

$$X_{\rm d} = (1 - d_\theta)(1 - d_{\hat\rho})X_0 = (1 - d_{\rm m})X_0 \tag{18}$$

Thus defining the moisture damage parameter $d_{\rm m}$ as

$$d_{\rm m} = d_\theta + d_{\hat\rho} - d_\theta d_{\hat\rho}; \quad 0 \leqslant d_{\rm m} \leqslant 1 \tag{19}$$

5. Simulation of combined physical–mechanical moisture damage

5.1. Finite element geometry and loading conditions

In this paper, the developed combined physical–mechanical moisture induced model is demonstrated on part of a micro-scale representation of the asphaltic pavement to demonstrate the importance of each of these moisture induced damage processes on the eventual developed damage pattern. In Fig. 7 the geometry and set-up of the finite element mesh is shown. The mesh consists of two stones, coated with a mastic film and a macro-pore which is saturated with moisture. The aggregate–mastic interface is also modelled to simulate the bond response. The macro-pore elements are simulated with a porous media formulation, which allows for the moisture to flow freely according to the formulations shown in the previous paper.

Even though the developed model is fully three dimensional, for demonstration purposes here only the two-dimensional response in the micro-scale finite element mesh is discussed.

Since the two aggregates are at the surface of the pavement, Fig. 7, they are in direct contact with the traffic loading. To simulate the tire–pavement interaction, a loading cycle is applied, which consists of 0.02 s pulses per tire, with 0.06 s period between the tires and 0.1 s between the next car loading. In the simulation, the loading of the stones, in time, is simulated with a compressive and shear pulse on the front and back side of the stones, with a time-lag of 0.01 s. In the simulation, traffic is assumed to move from the right to the left. The maximum applied compressive and shear stress is 0.7 MPa and 0.3 MPa, respectively. A complete loading cycle takes 0.2 s and is considered to be two wheel passes and one rest period (Fig. 8).

In the following, 13 different cases are simulated in which the diffusion of moisture, the erosion of mastic, the mechanical damage and the moisture susceptibility parameters are varied in a systematic way. These cases demonstrate that the consideration of physical moisture induced damage, together with mechanically generated damage, will lead to predictions of damage patterns which may differ considerable had they not been included. It furthermore shows the importance of determining the various moisture susceptibility parameters.

5.2. Moisture susceptibility parameters

In Table 1 the moisture susceptibility parameters of the various cases are summarized. In Case I–IV the moisture susceptibility coefficients concerning moisture diffusion are systematically varied for both the mastic and the aggregate–mastic interface. In these cases, additional damage to the mastic due to erosion or added mechanical damage due to the pumping action are not included.

In Case V–VIII the diffusion is not included, and the focus is entirely placed on the effect of the mechanical and physical damage due to the pumping action. Finally, in Case IX–XII both diffusion and pumping action

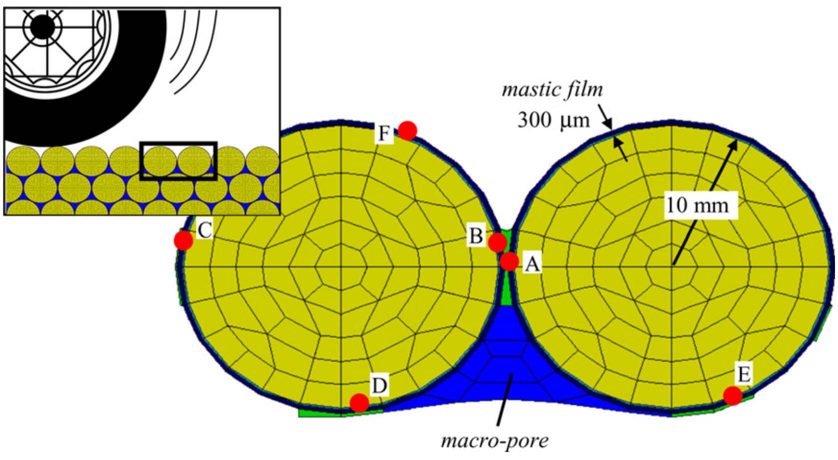

Fig. 7. Finite element mesh for the micro-scale analyses.

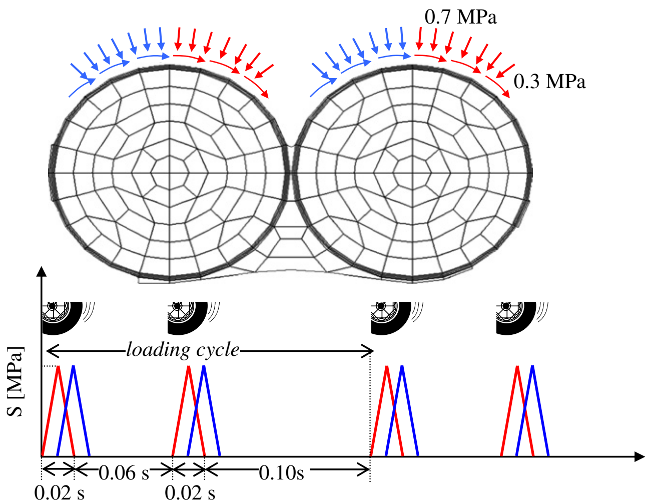

Fig. 8. Time scheme of applied loading cycle.

Table 1
Parametric simulation scheme

Case name	Moisture conditioning	Moisture susceptibility parameters	
		Mastic	Aggregate–mastic bond
Case 0: Dry	–	–	–
Case I: Diff	42 days diffusion	$D_{mst} = 3 \times 10^{-3}$ mm^2/h $\alpha_{\theta}^{mst} = 0.5$	$\alpha_{\theta}^{if} = 0.7$
Case II: Diff	42 days diffusion	$D_{mst} = 1.5 \times 10^{-2}$ mm^2/h $\alpha_{\theta}^{mst} = 0.5$	$\alpha_{\theta}^{if} = 0.7$
Case III: Diff	42 days diffusion	$D_{mst} = 1.5 \times 10^{-2}$ mm^{-2}/h $\alpha_{\theta}^{mst} = 0.0$	$\alpha_{\theta}^{if} = 1.2$
Case IV: Diff	42 days diffusion	$D_{mst} = 1.5 \times 10^{-2}$ mm^{-2}/h $\alpha_{\theta}^{mst} = 1.2$	$\alpha_{\theta}^{if} = 0.0$
Case V: Dry PA	PA (pumping action) No diffusion No erosion	$K_d = 0.0$ mm^3/g, $\alpha_{\hat{\rho}} = 0.0$	–
Case VI: Advec	PA and erosion No diffusion	$K_d = 1.0$ mm^3/g, $\alpha_{\hat{\rho}} = 2.0$	–
Case VII: Advec	PA and erosion No diffusion	$K_d = 1.0$ mm^3/g, $\alpha_{\hat{\rho}} = 5.0$	–
Case VIII: Advec	PA and erosion No diffusion	$K_d = 5.0$ mm^3/g, $\alpha_{\hat{\rho}} = 5.0$	–
Case IX: All	PA, erosion and 42 days diffusion	$K_d = 5.0$ mm^3/g, $\alpha_{\hat{\rho}} = 5.0$, $\alpha_{\theta}^{mst} = 0.5$ $D_{mst} = 1.5 \times 10^{-2}$ mm^2/h	$\alpha_{\theta}^{if} = 0.7$
Case X: All	PA, erosion and 42 days diffusion	$K_d = 1.0$ mm^3/g, $\alpha_{\hat{\rho}} = 5.0$, $\alpha_{\theta}^{mst} = 0.5$ $D_{mst} = 1.5 \times 10^{-2}$ mm^2/h	$\alpha_{\theta}^{if} = 0.7$
Case XII: All	PA, erosion and 42 days diffusion	$K_d = 1.0$ mm^3/g, $\alpha_{\hat{\rho}} = 5.0$, $\alpha_{\theta}^{mst} = 0.0$ $D_{mst} = 1.5 \times 10^{-2}$ mm^2/h	$\alpha_{\theta}^{if} = 1.2$
Case XI: All	PA, erosion and 42 days diffusion	$K_d = 5.0$ mm^3/g, $\alpha_{\hat{\rho}} = 5.0$, $\alpha_{\theta}^{mst} = 1.2$ $D_{mst} = 1.5 \times 10^{-2}$ mm^2/h	$\alpha_{\theta}^{if} = 0.0$

Table 2
Simulation parameters

Material	Visco-elastic component	Elasto-plastic component
Mastic	$E = 176$ MPa, $v = 0.3$ $\eta_d = 110$ MPa s, $\eta_v = 1000$ MPa s	$E = 176$ MPa, $v = 0.3$ $c_{y_0} = 0.12$ MPa, $c_{y_\infty} = 0.35$ MPa $\phi = 0.25$ rad, $\delta = 90$
Aggregate–mastic bond	$E = 100$ MPa, $v = 0.3$ $\eta_d = 70$ MPa s, $\eta_v = 1000$ MPa s	$E = 176$ MPa, $v = 0.3$ $c_{y_0} = 0.09$ MPa, $c_{y_\infty} = 0.35$ MPa $\phi = 0.15$ rad, $\delta = 90$

are included together. The original (undamaged) elasto-visco-plastic material properties of the stone, mastic and mastic–stone interface are kept equal in all cases and are summarized in Table 2. For the yield surface a standard Drucker–Prager formulation is used with a isotropic hardening which is controlled by δ:

$$c_y = c_{y_0} + \frac{\partial \psi}{\partial \xi} = c_{y_\infty} + (c_{y_0} - c_{y_\infty})\mathrm{e}^{-\delta \xi_p} \tag{20}$$

5.3. Analysis results

In Fig. 9 the complex shear stress field to which the mix is exposed to under the imposed loading cycles is shown. Over time, the imposed loading cycle is kept constant, however under the continued mechanical loading and moisture attack, the material properties are degrading differently at different locations and the stress and strain fields will be distributing differently, leading to various damage patterns.

For instance, the macro-pore between the two stones is simulated to be fully saturated with moisture. Due to the loading cycle, a water pressure is developing in the pore, which is exerting an added load on the areas connecting the macro-pore (Fig. 10). This cyclic pore pressure will induce added stresses and strains and therefore results in additional permanent deformations at certain locations, in addition to the mechanical loading which is directly applied on the top of the mesh. However, in addition to added mechanical damage, the building-up and reducing of pore pressure is also causing a pressure gradient in the water, which is locally causing

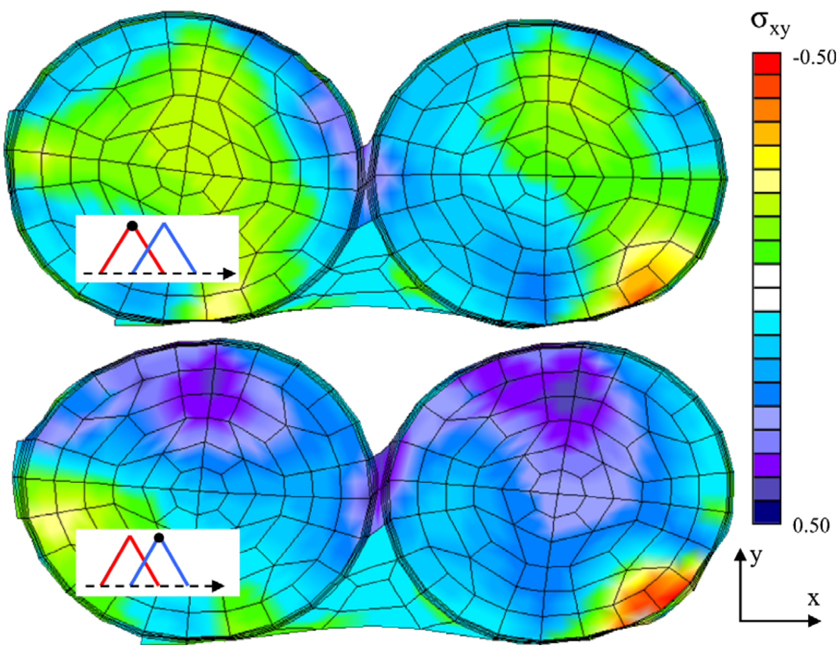

Fig. 9. Stress-xy development within the materials for Case II.

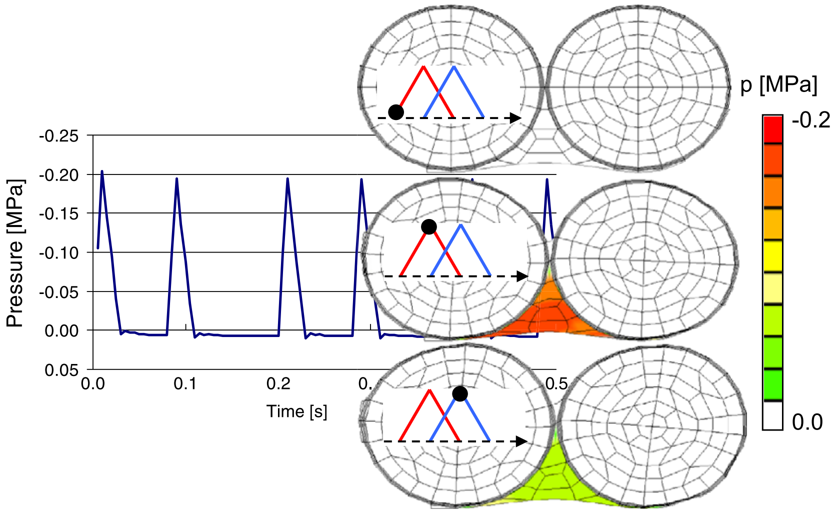

Fig. 10. Water pressure in the macro-pore.

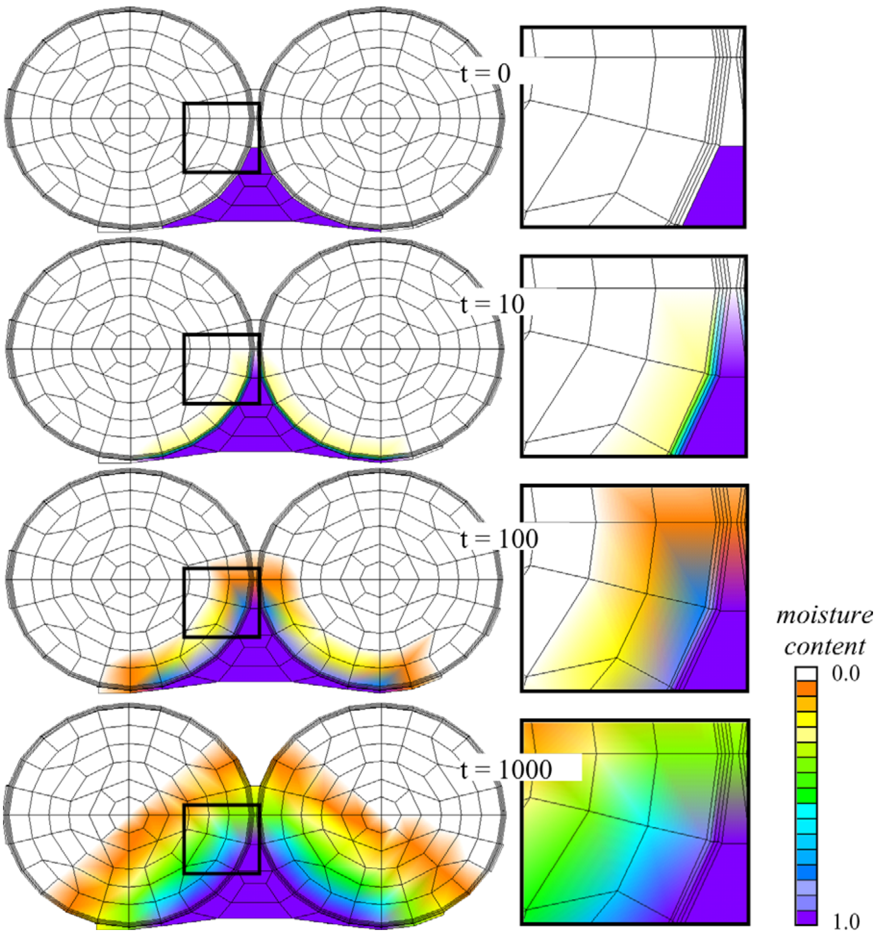

Fig. 11. Moisture diffusion simulation Case II, $D_{agg} = 0.01\ mm^2/h$ and $D_{mastic} = 0.015\ mm^2/h$.

fast water flow. As discussed earlier, depending on the desorption coefficient, the mastic film, which is in direct contact to the water in the macro-pore, will be subjected to an erosion effect, i.e. a diminishing mass density. Depending on the moisture susceptibility parameter, the erosion will locally cause a weakening of the material properties leading to additional plastic deformations.

Similarly, the moisture from the macro-pore will start diffusing slowly into the asphalt components, thereby locally weakening the material properties, Fig. 11. Since the moisture diffusion is a slower process than the mechanical loading cycles and the pumping action, in the analyses the mesh was preconditioned to 1000 h of moisture diffusion.

To characterize the developing damage patterns for the various simulation cases, a number of locations are selected for which the developing stresses and strains are outputted. In Fig. 7 an overview is given of these monitoring locations. An extensive comparison of the damage development in all monitoring locations for all 13 simulation cases is given in Kringos (2007). In the following only a few comparisons are highlighted to show the impact of the various moisture susceptibility parameters.

In Fig. 12 the stress–strain response of node A and D are plotted for Case 0 (dry), and diffusion Case II and Case III. What is first of all very noticeable from the comparison between the responses at these two locations is the entirely different, with the same loading conditions. This emphasizes the complexity of stress-states which different locations in the asphalt pavement will endure and also shows the importance of a generic constitutive model to capture this response. Secondly, in comparing the response of the two locations to the different moisture susceptibility cases, it becomes clear the at node A the Case II shows the greatest impact on the response and in node D it is Case III which has the biggest effect. In fact, this would mean that if the mix would consist of the moisture susceptibility parameters of Case II, the mix would most likely endure a cohesive mixture failure, whereas in Case III it would most like fail in an adhesive mode.

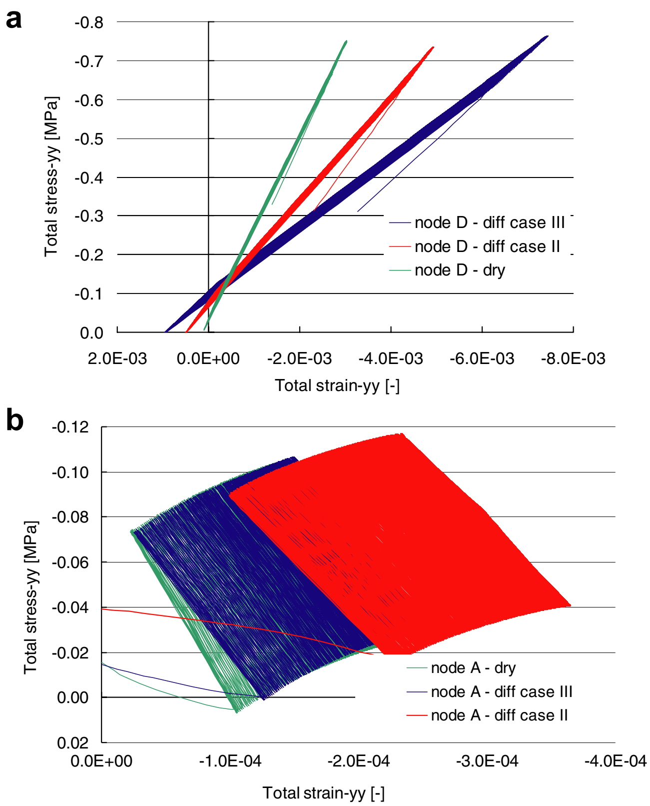

Fig. 12. Stress–strain response of node D and node A for Case 0, Case II and Case III for 3000 loading cycles.

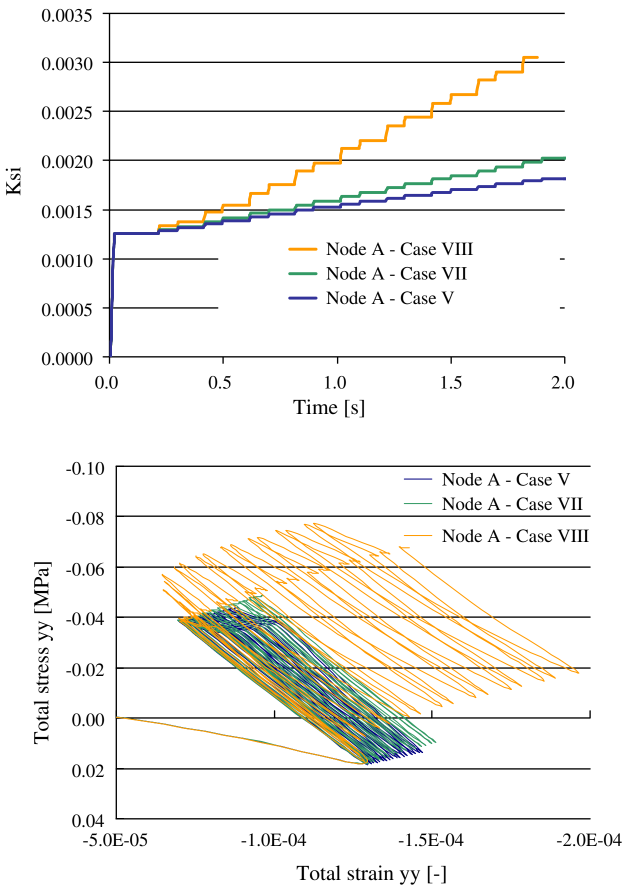

Fig. 13. Comparison response node A for Case V, VII and VIII.

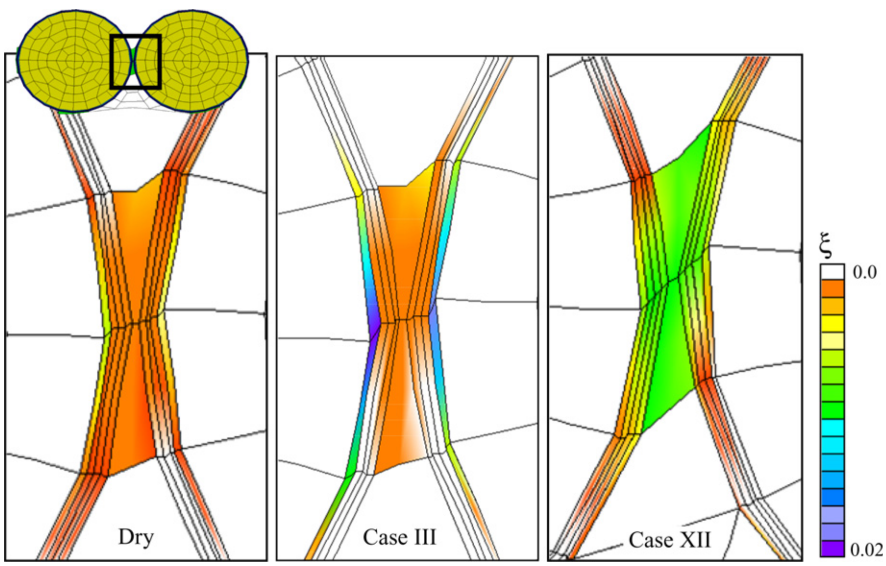

Fig. 14. Comparison of damage development for the various cases after 3000 loading cycles.

In Fig. 13 a comparison is made between the response of node A during the pumping action cases Case V, Case VII and Case VIII. The top graph shows the equivalent plastic strain development ξ_p, as described in the above, and the bottom graph shows the cyclic stress–strain response. As can be seen from Table 1 the difference between Case V and VI is and increased moisture susceptibility parameter $\alpha_{\hat{\rho}}$, with a constant desorption coefficient K_d. The difference between Case VI and VII is an increased desorption coefficient with a constant moisture susceptibility parameter. What becomes very clear from the comparison is that between Case V and VI, a slight increase in plastic deformation will occur in Node A and a small deterioration in the stress–strain response. However, in Case VIII the accumulation of plastic deformation rises quickly and the cyclic stress–strain response deteriorates dramatically. This shows that starting from an asphalt mix with the same mechanical material properties, the moisture susceptibility parameters could have a dramatic effect on the actual pavement performance and cause unexpected premature failure.

Finally, comparing the resulting permanent deformations after 3000 loading cycles in Fig. 14, for Case 0 (dry), Case III (diffusion) and Case XII (diffusion and pumping action), it can be seen that in Case III an adhesive failure in the aggregate–mastic interface would occur and in Case XII most likely a cohesive failure.

The performed computational analyses show the complexity of the stress–strain response at different locations in an asphaltic mix and indicate how physical and mechanical moisture susceptibility parameters influence the localized failure which may develop. It is therefore of paramount importance to measure the moisture susceptibility parameters to be able to predict if, when and where moisture would contribute to a premature weakening of the asphaltic pavement.

6. Conclusions and recommendations

The aim of this paper was to demonstrate the importance of various moisture susceptibility parameters of the asphalt mix components, on the overall response. To do so, several mechanical and physical damage processes were discussed and possible formulations of their damage functions were shown. Furthermore, by means of the newly developed finite element tool RoAM a demonstration was given of the effect of both physical and mechanical moisture damage inducing processes on a micro-scale representation of an asphaltic mix.

On the basis of this research, it is recommended that, in addition to the standard moisture susceptibility experiments which are currently performed, one starts determining the physical and physio-mechanical parameters discussed in this paper. A great benefit of such an approach would be that, instead of rejecting asphalt mixes because they fail an empirical test, one starts understanding which material property should be improved upon. The long-term benefit of this will be that, it becomes possible to 'engineer' the asphalt mixes, based on fundamental knowledge, rather than empirical speculations.

In addition to moisture, asphalt pavements are exposed to many other influences which may lead to damage (i.e. settlements, cracks, ageing etc.). It is therefore important in moisture damage susceptibility studies, either purely experimentally orientated ones or theoretically based ones, to always take into account the time frame over which moisture damage may be generated in comparison to other failures. If, for a particular mix, it is concluded that other damage failures are more likely to occur before moisture induced damage becomes an issue, focus should be placed on improving the dominant material parameters which control these, and less effort should be spend to improve the moisture susceptibility characteristics of the mix. An estimate of the time frame over which moisture damage may occur can be made with the presented tools.

Finally, it can be concluded from the computational analyses that the identified moisture susceptibility parameters can be of paramount importance to the resulting failure pattern. Determination of the dominant moisture susceptibility material parameters which where identified in this research, can lead to better failure predictions and improved asphalt mixtures.

Acknowledgements

The authors thank Dr. A. de Bondt of Ooms Nederland Holding Bv in the Netherlands for the financial and experimental support of the RAVEMOD project.

References

Copeland, A., Kringos, N., Scarpas, A., Youtcheff, J., 2007. Determination of combined physical–mechanical moisture induced damage in the aggregate–mastic bond. In: Proceedings of the International Conference on Advanced Characterisation of Pavement and Soil Engineering Materials, Athens, Greece.

Curtis, C.W., Ensley, K., Epps, J., 1991. Fundamental properties of asphalt aggregate interactions including adhesion and adsorption, SHRP A-003B.

Fromm, H.J., 1979. The mechanism of asphalt stripping from aggregate surfaces. Journal of the Association of Asphalt Paving Technologists 43.

Graf, P., 1986. Factors affecting moisture susceptibility of asphalt concrete mixtures. Journal of the Association of Asphalt Paving Technologists 55.

Hicks, R.G., 1991. Moisture Damage in Asphalt Concrete, NCHRP Synthesis of Highway Practice 175, TRB, NRC.

Ishai, I., Craus, J., 1972. Effect of filler on aggregate–bitumen adhesion properties in bituminous mixtures. Journal of the Association of Asphalt Paving Technologists 41.

Kanitpong, K., Bahia, H., 2003. Role of adhesion and thin film tackiness of asphalt binders in moisture damage of HMA. Journal of the Association of Asphalt Paving Technologists 72.

Kandhal, P., 1992. Moisture susceptibility of HMA mixes: identification of problem and recommended solutions. NCAT Report 92-1.

Kandhal, P., 1994. Field and lab investigation of stripping in asphalt pavements: state-of-the-art. Transportation Research Record: Journal of the Transportation Research Board 1454, NRC.

Kandhal, P., 2001. Premature failure of asphalt overlays from stripping: case histories. Journal of the Association of Asphalt Paving Technologists 70.

Kringos, N., Scarpas, A., 2005. Ravelling of asphaltic mixes: computational identification of controlling parameters. Transportation Research Record: Journal of the Transportation Research Board, No. 1929, Bituminous Paving Mixtures, 79–87.

Kringos, N., Scarpas, A., Kasbergen, C., 2007a. Three dimensional elasto-visco-plastic finite element model for combined physical–mechanical moisture induced damage in asphaltic mixes. Journal of the Association of Asphalt Paving Technologists 76.

Kringos, N., Scarpas, A., Selvadurai, A.P.S., 2007b. Simulation of mastic transport from open graded asphalt mixes using a hybrid Lagrangian–Eulerian finite element. In: Proceedings of the International Conference on Advanced Characterisation of Pavement and Soil Engineering Materials, Athens, Greece.

Kringos, N., 2007. Modeling of combined physical–mechanical moisture induced damage in asphaltic mixes. Ph.D. Dissertation, Delft University of Technology, ISBN 978-90-9021765-9.

Kringos, N., Scarpas, A., Bondt de, A., 2008a. Determination of moisture susceptibility of mastic-stone bond strength and comparison to thermodynamical properties. Journal of the Association of Asphalt Paving Technologists 77.

Kringos, N., Scarpas, A., Selvadurai, A.P.S., 2008b. Modeling of combined physical–mechanical moisture induced damage in asphaltic mixes, Part 1: governing processes and formulations. International Journal for Pavement Engineering 2.

Lytton, R., 2002. Mechanics and measurement of moisture damage. In: Proceedings of Moisture Damage Symposium, WRI, Wyoming, July.

Majidzadeh, K., Brovold, F., 1968. State-of-the-art: effect of water on bitumen–aggregate mixtures. HRB Special Report No. 98.

Mcgennis, R.B., Kennedy, T.W., Machemehl, R., 1984. Stripping and moisture damage in asphalt mixtures. FHWA Report TX 85, Dept. of Highways and Public Transportation, Texas.

Riedel, W., Weber, H., 1953. On the adhesiveness of bituminous binders on aggregates. Asphalt and Tar.

Reese, S., Govindjee, S., 1998. A theory of finite viscoelasticity and numerical aspects. International Journal of Solids and Structures 35, 3455–3482.

Scarpas, A., 2000. CAPA-3D Finite Element System Users Manual I, II and III. Delft University of Technology Publication.

Scarpas, A., Kasbergen, C., Kringos, N., 2005. Course Notes, International Course on Advanced Constitutive Modeling of Asphaltic Materials, January 2005, MD, USA.

Scarpas, A., 2005. A Mechanics based computational platform for pavement engineering, ISBN 90-9019040-6.

Scarpas, A., Kasbergen, C., 2006. An energy based constitutive framework for modeling of asphalt concrete: theoretical, experimental, and numerical aspects. In: Proceedings of Geocongress "Geotechnical Engineering in the information Technology Age", Atlanta. American Society of Civil Engineers, ISBN 0-7844-0803-3.

Scholz, T.V., Terrel, R.L., Al-Joaib, A., Bea, J., 1993. Water sensitivity: binder validation. Report SHRP-A-402, NRC.

Scott, J.A., 1978. Adhesion and disbonding mechanisms of asphalt used in highway construction and maintenance. Journal of the Association of Asphalt Paving Technologists 47.

Stuart, K., 1990. Moisture damage in asphalt mixtures – state-of-the-art. Report FHWA-RD-90-019, FHWA, VA 22101-2296.

Takkalou, H.B., 1984. Stripping of asphalt pavements: state-of-the-art. Transportation Research Record: Journal of the Transportation Research Board, 84-6.

Taylor, M.A., Khosla, N.P., 1983. Stripping of asphalt pavements: state-of-the-art. Transportation Research Record: Journal of the Transportation Research Board, 911.